Liver slice culture as a model for lipid metabolism in fish

Thomas N Harvey [1], **Simen R Sandve** [1], **Yang Jin** [1], **Jon Olav Vik** [Corresp., 1], **Jacob S Torgersen** [Corresp. 2]

[1] Centre for Integrative Genetics (CIGENE), Department of Animal and Aquacultural Sciences, Faculty of Biosciences, Norwegian University of Life Sciences, Ås, Norway

[2] Torgard, Aquagen AS, Trondheim, Norway

Corresponding Authors: Jon Olav Vik, Jacob S Torgersen
Email address: jonovik@gmail.com, jactor@aquagen.no

Hepatic lipid metabolism is traditionally investigated *in vitro* using hepatocyte monocultures lacking the complex three-dimensional structure and interacting cell types essential liver function. Precision cut liver slice (PCLS) culture represents an alternative *in vitro* system, which benefits from retention of tissue architecture. Here we present the first comprehensive evaluation of the PCLS method in fish (Atlantic salmon) and validate it in the context of lipid metabolism using feeding trials, extensive transcriptomic data, and fatty acid measurements. We observe an initial period of post-slicing global transcriptome adjustment, which plateaued after three days in major metabolic pathways and stabilized through nine days. PCLS fed alpha-linolenic acid (ALA) and insulin responded in a liver-like manner, increasing lipid biosynthesis gene expression. We identify interactions between insulin and ALA, where two PUFA biosynthesis genes that were induced by insulin or ALA alone, were highly down-regulated when insulin and ALA were combined. We also find that transcriptomic profiles of liver slices are exceedingly more similar to whole liver than hepatocyte monocultures, both for lipid metabolism and liver marker genes. PCLS culture opens new avenues for high throughput experimentation on the effect of “novel feed composition” and represent a promising new strategy for studying genotype-specific molecular features of metabolism.

Liver slice culture as a model for lipid metabolism in fish

Thomas N. Harvey[1], Simen R. Sandve[1], Yang Jin[1], Jon Olav Vik[1]*, Jacob S. Torgersen[2]*

[1] Centre for Integrative Genetics (CIGENE), Department of Animal and Aquacultural Sciences, Faculty of Biosciences, Norwegian University of Life Sciences, NO-1432 Ås, Norway

[2] AquaGen AS, Postboks 1240, Torgard, NO-7462 Trondheim, Norway

*shared corresponding author

Corresponding authors:

Jon Olav Vik, Ph.D., Centre for Integrative Genetics (CIGENE), Department of Animal and Aquacultural Sciences, Faculty of Biosciences, Norwegian University of Life Sciences, NO-1432 Ås, Norway, jonovik@gmail.com, +47 4588 2998

Jacob S. Torgersen, Ph.D., AquaGen AS, Postboks 1240, Torgard, NO-7462 Trondheim, Norway, jactor@aquagen.no, +47 9201 9966

Abstract

Hepatic lipid metabolism is traditionally investigated *in vitro* using hepatocyte monocultures lacking the complex three-dimensional structure and interacting cell types essential for liver function. Precision cut liver slice (PCLS) culture represents an alternative *in vitro* system, which benefits from retention of tissue architecture. Here we present the first comprehensive evaluation of the PCLS method in fish (Atlantic salmon) and validate it in the context of lipid metabolism using feeding trials, extensive transcriptomic data, and fatty acid measurements. We observe an initial period of post-slicing global transcriptome adjustment, which plateaued after three days in major metabolic pathways and stabilized through nine days. PCLS fed alpha-linolenic acid (ALA) and insulin responded in a liver-like manner, increasing lipid biosynthesis gene expression. We identify interactions between insulin and ALA, where two PUFA biosynthesis genes that were induced by insulin or ALA alone, were highly down-regulated when insulin and ALA were combined. We also find that transcriptomic profiles of liver slices are statistically more similar to whole liver than hepatocyte monocultures after 5 days, both for lipid metabolism and liver marker genes. PCLS culture opens new avenues for high throughput experimentation on the effect of "novel feed composition" and represent a promising new strategy for studying genotype-specific molecular features of metabolism.

Introduction

Liver is the metabolic transformation hub. It is responsible for receiving nutrients absorbed in the gut through the portal vein, processing these nutrients for storage or energy production, and subsequent transportation of metabolic products throughout the body. Essential to proper function, the complex three-dimensional structure of liver consists of intrahepatic microcirculatory units (lobules) of tightly associated cells that communicate through paracrine and autocrine effects (Wake & Sato, 2015). The liver is also the main organ for detoxification, so *in vitro* methods are commonly applied for toxicological studies to reduce use of *in vivo* experiments. Hepatocyte cultures were established in the 1970s (Ekins, 1996), and rapidly became the preferred model system for toxicology. Liver slice culture was first introduced in 1923 (Warburg, 1923), but seldom used due to a lack of reproducibility since slices needed to be cut by hand.

The development of automated tissue slicers in the 1980s (Krumdieck, Dos Santos & Ho, 1980) solved this problem, so liver slices became a viable option. One of the main advantages of liver slices is the retention of normal cell composition and 3D structure. In addition, the preparation is fast, reproducible, without enzymatic cell dissociation, and no need for coating the growth surface. Together with established protocols, this has heralded the return of liver slices for *in vitro* studies.

Precision cut liver slice (PCLS) cultures have been applied in a number of toxicology studies and most recently also immunology (Wu et al., 2018), however the use of PCLS to study central liver metabolism is sparse, with few PCLS studies investigating aspects of lipid metabolism, all of which are in mammals (Neyrinck, Gomez & Delzenne, 2004; Szalowska et al., 2014; Janssen et al., 2015; Fortin et al., 2017). We provide a critical evaluation of PCLS as a metabolic model system in fish by characterizing whole transcriptome changes in the context of lipid metabolism. We chose Atlantic salmon for its economic importance; and because development of feeding and breeding strategies that optimize omega-3 production require a better understanding lipid metabolism. Additionally, the effect of altered feed fatty acid profile on liver gene expression is well documented (Tocher et al., 2001; Leaver et al., 2008; Gillard et al., 2018) making this an ideal system for assessing the effects of altering media fatty acid composition and comparing to expected *in vivo* gene expression.

Here we integrate transcriptomics data with domain knowledge to describe a method for using PCLS as a model system to study lipid metabolism. We aim to 1) characterize transcriptome wide changes in liver slice culture over time, 2) demonstrate the utility of using liver slice culture to study lipid metabolism, and 3) compare gene expression patterns between liver slice culture, 2D hepatocyte culture, and whole liver *in vivo*.

Materials and Methods

Liver slice culture

Atlantic salmon used in this study were sacrificed according to the Norwegian Animal Research Authority (NARA); regulations for use of experimental animals (FOR-2015-06-18-761). The liver was removed immediately after euthanization and placed in ice cold Hank's balanced salt solution (HBSS, Thermofisher). Livers were cut into approximately 4 mm x 4 mm x 8 mm strips before being superglued to a plastic piston and encased in ultra-low melt agarose (Merck). Liver strips were sliced to a thickness of 300 µm using a compresstome VF-300 (Precisionary Instruments) and collected in ice cold HBSS before being transferred to 15°C Leibovitz 15 medium pH 7.4 (L15, Thermofisher) containing 5% fetal bovine serum (FBS, Merck) and 1% penicillin - streptomycin (PS, Thermofisher) which will now be referred to as base media. Liver slices were incubated in sterile 6 (2mL media per well) or 12 (4mL media per well) well cell culture plates with netwell inserts (Corning, 500 µm membrane size) for up to 9 days at 15°C under ambient air. For each of the following experiments, liver slices were prepared from a single fish each time to eliminate biological variation.

Time course experiments

We performed two time course experiments, the first to test the effect of culturing time on the liver slices, and the second as a follow up to test the effect of media change frequency and inclusion of insulin over time. In both experiments, liver slices were generated immediately after euthanization and viability measurements were taken every day in the first experiment and on days three and six in the second experiment. All samples were stored in RNAlater at -20℃. In the first experiment we generated slices from a saltwater life-stage Atlantic salmon (~200g) reared on a marine oil based diet high in DHA and EPA. Immediately after euthanization, liver slices were generated as described above. Media was changed on days three and six using base media supplemented with 700 µM randomly methylated beta cyclodextrin (BCD) and 0.7% ethanol. Samples were taken in triplicate before slicing (whole liver) and 1, 3, 4, 5, 6, 7, 8, and 9 days after slicing. In the second time course experiment we used Atlantic salmon in the freshwater life-stage reared on a marine oil diet high in EPA and DHA. Human insulin (Merck) was included in the media at 20 nM and media was refreshed either every day or every third day with fresh base media

containing 20nM insulin. Samples were taken in triplicate before slicing (whole liver) and days 3, 4, 5, 6, 7, 8, and 9.

Fatty acid and insulin gradient experiments

We performed two concentration gradient experiments, the first was used for transcriptomic analysis, the second for fatty acid analysis. In the first experiment liver slices were prepared from two freshwater stage Atlantic salmon (~50g), one for use in the fatty acid gradient experiment and one for use in the insulin gradient experiment. We used randomly methylated beta-cyclodextrin (BCD) as our fatty acid delivery system since it has been demonstrated to efficiently deliver fatty acids across membranes in other *in vitro* systems (Brunaldi, Huang & Hamilton, 2010). Alpha-linolenic acid (ALA) was stored at 10mM in ethanol then mixed 1:1 with 100mM BCD in water for a final molar ratio of 1:10 fatty acid to BCD. From this stock ALA was added to the media at a concentration of 0 (BCD only), 20, 40, 70, and 100 µM, aliquoted into a new six well culture plate, and placed at 15°C to equilibrate for at least 30 minutes. For all ALA treated samples, liver slices were transferred to ALA supplemented base media after a three day recovery period. For the insulin containing samples, human insulin (Merck) was diluted in base media to a final concentration of 10 or 100nM and incubated with liver slices from the beginning of the experiment. All liver slices were sampled in triplicate on day five and stored in RNAlater at -20℃. In the second concentration gradient experiment, liver slices were prepared from freshwater stage fish (~500g) and supplemented with 0 (BCD only), 20, 40, 70, 100, and 140µM ALA on day three as described except this time ethanol was evaporated under a stream of nitrogen before mixing with BCD. Samples were taken in triplicate on day four, washed in ice cold HBSS, flash frozen in an ethanol dry ice slurry, and stored at -80℃.

2D hepatocyte culture experiment

Primary cells were isolated from salmon liver as described (Bell et al., 1997), with some modifications. After euthanization, the liver was removed and rinsed in ice cold Mg2+/Ca2+ free HBSS, before ~100 ml of the same buffer was directly injected with a 50 ml syringe and 27G needle, at various places to wash out blood cells. Then, 30 ml of HBSS with 150U/ml Collagenase type 1 (Merck) was injected, before the tissue

was finely chopped. The tissue suspension was incubated for 1h at 10-12°C with agitation. Dissociated cells were collected by cell straining (70 µm) and centrifugation for 10 min at 100g. After three washes in HBSS, the pellet was resuspended in base media supplemented with 10 µM human insulin (Merck) and grown at 200k/cm^2 density at 15°C on polyethyleneimine coated wells (Vancha et al., 2004). Cells were supplemented with ALA on day five as previously described and collected in triplicate using a cell scraper on days five (before ALA), six, and eight by flash freezing and storing at -80°C.

Viability measurement

Slice viability was assessed by staining with Hoechst and propidium iodide to identify live and dead cells. Slices were transferred to L15 medium containing 10µg/mL Hoechst and 10µg/mL propidium iodide for 5 minutes at 15°C. Slices were then transferred to fresh L15 medium and placed on ice until being imaged with a scanning laser confocal microscope (CLSM, Leica). Live/dead ratios were determined using Icy (http://www.bioimageanalysis.org/). We compared the proportions of live and dead cells in two randomly selected locations per slice to determine overall slice viability.

Microscopy

We made cross sections of liver slices at three different time points during culturing (one slice per time point) and observed morphological changes using light microscopy. All samples for microscopy were fixed using 4% formalin in phosphate buffered saline (PBS) for 1 hour then transferred to 70% ethanol stepwise (PBS-25%-50%-70%) for 5 minutes at each step and stored at -20°C until microscopic analysis was performed. Prior to paraffin embedding liver slices were transferred to 96% ethanol stepwise (70%-85%-96%-96%) for 5 minutes at each step then washed twice with histoclear (National diagnostics) for 5 minutes each. Next, liver slices were embedded in paraffin (Merck) by incubating in paraffin at 61°C three times for 10 minutes each. Paraffin was allowed to solidify at room temperature. Liver slice cross-sections were prepared using a rotary microtome (Leica) at a thickness of 7µm, placed on the surface of a 43°C water bath, and floated onto a clean microscopy slide. Sections were deparaffinized by washing twice with histoclear for 5 minutes each and rehydrated by transferring to 70% ethanol stepwise (histoclear-96%-85%-70%-70%) for 5 minutes each followed by a brief wash in distilled water. Sections were stained with a 1%

hematoxylin solution (Mayer's) for eight minutes, rinsed in running tap water for 10 minutes followed by 96% ethanol and counterstained with a 0.25% eosin-phloxine B solution for 30 seconds. Stained sections were washed twice with histoclear for five minutes each and mounted with DPX (Merck). Micrographs of cross-sections were taken at 20x magnification on a light microscope (Leica).

RNA sequencing

Slices were stored in RNAlater (Merck) at -20°C until RNA extraction using the RNeasy universal kit (QIAGEN). RNA concentration was determined on a Nanodrop 8000 and quality was determined on an Agilent 2100 bioanalyzer using Agilent RNA 6000 nano chips. All RNA samples had a RNA integrity number greater than 7. mRNA libraries were prepared using the Trueseq library preparation kit (Agilent). Concentration and mean length were determined by running cDNA libraries on a bioanalyzer 2100 using DNA 1000 chips (Agilent). RNA libraries were sequenced on an Illumina HiSeq 2500 with 100-bp single end reads.

RNAseq analysis

All RNA sequencing and demultiplexing was done at the Norwegian sequencing center (Oslo, Norway). Fastq files were trimmed and mapped the the salmon genome (ICSASG_v2) using STAR (v2.5.2a) (Dobin et al., 2013). Mapped reads for each gene were counted with HTSeq-count (v0.6.1p1) (Anders, Pyl & Huber, 2015). Differential expression analysis was performed in R (v3.2.5) using the edgeR package (Robinson, McCarthy & Smyth, 2010). All counts were normalized to library size using TMM normalization within edgeR. For the time course and gradient experiments an ANOVA-like differential expression test was used to find difference between any of the conditions (see edgeR manual). This yielded log2 fold change to the reference level (day0 or ALA0) and false discovery rate (FDR) for each gene. For the time course experiments we considered genes with a FDR of <0.01 and log2FC >1 as differentially expressed while for the gradient experiments genes with a FDR of <0.01 were considered differentially expressed. Gene expression clusters were generated by applying wardD2 hierarchical clustering to gene-scaled mean counts per million. KEGG enrichment was performed on each gene cluster using edgeR. Pathways with a p-value <0.001 were considered significantly enriched. To compare gene expression

between whole liver, liver slice, and hepatocyte culture, we pooled data from each source to give an overall expression phenotype. Data on whole liver was obtained from a previously published feeding trial (Gillard et al., 2018) and whole liver samples taken before generating liver slices. Data on liver slice and hepatocyte culture was obtained from the previously described experiments.

Lipid analysis

Fatty acid methyl esters (FAME) were prepared from liver slices according to established protocols (O'Fallon et al., 2007) with half volumes to account for the small size of liver slices. We used 13:0, 19:0, and 23:0 as an internal standards in all samples and FAMEs were separated by gas chromatography on a Trace GC Ultra (Thermo Scientific) using a flame ionization detector. Relative fatty acid abundance was calculated from the resulting chromatograms.

Statistical analysis

All statistical analysis was performed in R (v3.2.5). Correlation analysis between whole liver and liver slice samples was calculated using the mean counts per million (CPM) of each gene across the three time course experiments (whole liver) and triplicate samples within each experiment (liver slice) for each day followed by Spearman's rank correlation test. Comparison of gene expression (CPM) between groups in the ALA and insulin gradient experiments was calculated using a one-way analysis of variance (ANOVA) test followed by a Tukey-HSD test. Differences with a p-value <0.05 were considered significant.

Results

Viability and morphology

Liver slices were highly viable in all experiments with a mean viability of 90.3±2.7% (Fig. 1B). We did not observe any viability effects of ALA, insulin nor methyl-β-cyclodextrin (BCD) used as a lipid carrier in the experiments. More generally, we find that viability at the end of an experiment is similar to the viability at the beginning of an experiment (Fig. 1B). This implies that preparation of the slices is most critical to viability, as opposed to culture time. Morphological analysis of liver slice cross-sections did not reveal any large change in the thickness of slices over a five day period. Slices did appear thinner than they were cut

(300 μM), but this is likely due to dehydration causing the liver slices to shrink during the paraffin embedding process (Fig. 1C). Slices examined were approximately 188 μm, 183 μm, and 210 μm in thickness on days 0, 3, and 5, respectively.

Time course experiments

In order to study how the liver slices change in culture over time, we sequenced RNA from three experiments lasting for nine days. In time course one, media was changed every three days and samples were taken before slicing (day 0) and 1, 3, 4, 5, 6, 7, 8, and 9 days after slicing. On day three, slices were fed a control diet consisting of BCD only. We use BCD to deliver the fatty acids to the cells, so in this case BCD only was used as a control for fatty acid supplementation conditions. The second and third time course experiments differed from the first in terms of media change frequency (daily or every third day) and inclusion of insulin in the media (20nM).

To characterize the behavior of liver slices over time under control conditions, we performed ANOVA-like differential expression analysis testing for differentially expressed genes between any of the time points in time course one. This yielded 16,267 differentially expressed genes (DEG) with a false discovery rate (FDR) < 0.01 and a log2 fold change (log2FC) >1 (Fig. 2A). We used hierarchical clustering to group genes with a similar expression trend into eight gene clusters (Fig. 2B), then searched for enriched pathways from the Kyoto encyclopedia of genes and genomes (KEGG) in each of these clusters ($p < 0.0001$) to characterize the overall trend of various physiological and metabolic processes (Fig. 2C). Interestingly, almost all pathways related to protein, lipid, carbohydrate and vitamin metabolism belong to clusters two and three, which decreased between day zero (before slicing) and day three, followed by an overall stabilization in expression through day nine. Pathways related to signal transduction were mostly enriched in clusters seven and eight, which increased expression greatly between day zero and day one (before and 24 hours after slicing), then decreased to original levels by day 9. Pathways related to cell growth and death were mostly enriched in clusters four, five, and six, which in general increased during 9 days of liver slice culture.

Since cell culture aims to mimic the conditions and behavior of tissue *in vivo*, we compared gene expression patterns between whole liver and liver slices for all three experiments. To assess the similarity in expression patterns over time we calculated Spearman co-expression correlations between mean whole liver gene expression and gene expression from each day in three time course experiments for all genes and genes within seven relevant lipid metabolism pathways (Fig. 3). For time course one, correlation between liver slices and whole liver decreased gradually over time from 0.90 on day 1 to 0.83 on day 4, then stabilized around 0.8 through day 9. A similar effect was observed in time course two and time course three with co-expression correlation to whole liver stabilizing around 0.82 through day 8 then decreasing to 0.78 and 0.79 respectively on day 9 (Fig. 3). The greatest difference between whole liver and liver slices was in the pathway "*Steroid biosynthesis*" with co-expression correlations hovering between 0.48 and 0.28 during days three through nine for all three experiments. Co-expression correlation was slightly more stable over time when media was refreshed daily, especially "*Steroid biosynthesis*"; however, overall expression similarity to whole liver was high for nearly all pathways and time points examined.

Fatty acid and insulin gradient experiments

In order to evaluate fatty acid uptake and transcriptomic response in liver slices, we added alpha-linolenic acid (ALA) to the media in increasing concentrations from 20µM up to 100µM. We expect this to trigger upregulation of lipid metabolism-related gene expression as observed in liver of fish fed vegetable oil diets high in ALA (Gillard et al., 2018). ANOVA-like differential expression analysis testing for differences between any of the ALA concentrations yielded 8,282 DEGs (FDR < 0.01, Fig. S1A). We then broke these DEGs into four expression clusters as previously explained (Fig. S1B). KEGG enrichment analysis on these four clusters yielded 37 total pathways significantly enriched ($p < 0.001$) in one or more cluster (Fig. S1C). We found that all enriched pathways relating to lipid metabolism belonged to the same cluster which increased with increasing ALA concentration, especially between 40 and 70µM. Specifically, the pathways *"biosynthesis of unsaturated fatty acids"*, *"fatty acid degradation"*, *"glycerolipid metabolism"*, *"steroid biosynthesis"*, and *"PPAR signaling pathway"* were all enriched in this cluster (Fig. S1B and C).

247

248 In order to better characterize the effect of ALA supplementation on PUFA biosynthesis, we analyzed
249 individual gene expression of key genes in the PUFA biosynthesis pathway (Fig. 4). The five key genes
250 involved in PUFA biosynthesis that are differentially expressed at some point in the ALA concentration
251 gradient include delta-5 desaturase (*Δ5fad*), delta-6 desaturase a (*Δ6fada*), fatty acid elongase 2 (*elovl2*),
252 fatty acid elongase 5a (*elovl5a*), and fatty acid elongase 5b (*elovl5b*). All five genes displayed an overall
253 positive correlation with ALA concentration (Fig. 4B) with *Δ5fad*, *Δ6fada*, and *elovl2* responding strongly
254 to ALA between 40μM and 70μM and both *elovl5* genes less influenced, slightly increasing with increasing
255 ALA concentration. Counterintuitively, at low ALA concentration (20μM) all genes except *elovl2* and
256 *elovl5a* significantly decreased ($q<0.05$) in expression compared to control samples (no fatty acid). Between
257 70μM and 100μM ALA, expression of *Δ5fad*, *Δ6fada*, and *elovl2* did not significantly change (Fig. 4B).

258

259 To assess the impact of ALA supplementation (up to 140μM) on the fatty acid profile of liver slices we
260 conducted a second ALA concentration gradient experiment. As expected, percent ALA increased with
261 increasing media ALA concentration from 0.87% with no ALA supplementation to 6.5% with 140μM ALA
262 supplementation (Fig. 4C). In addition, the elongation product of ALA, 20:3n-3, increased with increasing
263 media ALA concentration from 0.35% with no ALA supplementation to 2.7% with 140μM ALA
264 supplementation (Fig. 4C). EPA and DHA levels do not significantly ($q<0.05$) change at any point in the
265 ALA gradient (Fig. 4C). There was a large difference in proportions of 18:0, EPA, and DHA between fresh
266 liver and liver slices after four days of incubation (tables S1 and S2). 18:0 doubled, increasing from 5.8%
267 in fresh liver to 12.3% in liver slices. Both EPA and DHA decreased in liver slices, from 6.4% to 3.5% and
268 29.6% to 25.1%, respectively (table S1).

269

270 The effect of insulin supplementation on liver slices was assessed by incubating slices with two different
271 concentrations of insulin, 10nM and 100nM. To test for an interaction between insulin and fatty acid

supplementation, we also tested these insulin levels with and without supplementation of 70μM ALA. Differential expression analysis testing for changes in expression between any of the conditions (without ALA supplementation) yielded 11,898 DEGs (FDR <0.01, Fig. S2A). Approximately half of these genes were upregulated (5,889 DEGs) and half were downregulated (6,012 DEGs) regardless of insulin concentration (Fig. S2B). Only 13 genes were differentially expressed between the two insulin concentrations. KEGG pathway enrichment on these gene clusters revealed that most metabolism related pathways were upregulated with the addition of insulin. Specifically relating to lipid metabolism, "*biosynthesis of unsaturated fatty acids*", "*fatty acid biosynthesis*", and "*PPAR signaling pathway*" were significantly enriched in the upregulated gene set (Fig. S2C). Pathways related to metabolism enriched in the downregulated gene set included "*glycerophospholipid metabolism*", "*inositol phosphate metabolism*", and interestingly "*insulin signaling pathway*" (Fig. S2C).

Insulin supplementation alone tended to increase expression of key PUFA biosynthesis genes except for *Δ5fad*, which did not significantly (q<0.05) change with increasing insulin concentration (Fig. 4D). Increasing insulin concentration from 10nM to 100nM did not significantly change the expression of any of the five genes. Addition of 70μM ALA had a large effect on the expression of *Δ5fad* and *Δ6fada*, which were expressed most in the absence of insulin, then downregulated upon insulin supplementation. ALA supplementation did not appear to have a large effect on the expression of *elovl5a* and *elovl5b*, which agrees with findings from the ALA gradient experiment.

Liver slice culture versus primary cell culture

To assess how liver slice culture compares to widely used hepatocyte culture and liver *in vivo*, we compared RNA sequencing data from hepatocyte culture (n = 16 from one fish), liver slice culture (n = 89 from four fish), and whole liver (n = 210 from 210 fish). Hepatocytes were sampled after 5, 6, and 8 days in culture, so only liver slices incubated at least 5 days were used for comparison. The hepatocytes displayed a cuboidal morphology and we did not find an increase in the expression of the viability marker apoptosis inducing factor 1 (*aif1*, Fig S3) or a reduction in RNA quality or abundance over time, indicating that primary

hepatocytes remained healthy after 8 days in culture. Data on whole liver was obtained from a feeding trial where salmon were fed either a fish oil or plant oil based diet (Gillard et al., 2018). All data from each source was pooled to give a range of possible expression patterns from that source. We then calculated relative expression by scaling expression of each gene across all data sources.

We find that overall, liver slice culture more closely resembles whole liver than hepatocyte culture. Gene expression in the lipid related KEGG pathways *"fatty acid biosynthesis"*, *"glycerolipid metabolism"*, *"biosynthesis of unsaturated fatty acids"*, and *"steroid biosynthesis"* was much lower in hepatocyte culture relative to both liver slice culture and whole liver (Fig. 5A). This was reflected in the expression of all underlying key PUFA biosynthesis genes except *elovl5a* (Fig. 5B). Expression of genetic marker genes characteristic of functional liver was generally lower in hepatocyte culture, while liver slice culture was closer, but not identical to whole liver expression patterns (Fig. 5C). Specifically, albumin genes *alb1*, *alb2-1*, and *alb2-2* and glucose-6-phosphatase genes *g6pcl-3* and *g6pcl-4* had lowest expression in hepatocyte culture followed by liver slice culture and highest expression in whole liver (Fig. 5C).

Discussion

Liver slice metabolism stabilizes after three days and remains liver-like through nine days in culture

We find that time, up to 9 days tested, does not have a large effect on the viability or thickness of the slices. This is encouraging, since morphometric analysis of Atlantic cod liver slices showed an increase in the proportion of dead cells at 72 hours in culture (Eide et al., 2014) and studies on rat liver slices have shown that changes in viability and slice thickness over time is highly dependent on the culture media used (Starokozhko et al., 2015).

We do, however, observe a time dependent drift in gene expression patterns. Slices most resemble whole liver 24 hours after slicing with a correlation coefficient of 0.90 and gradually decrease in similarity over

time (Fig. 3). A similar effect has been observed in rat liver slices (Boess et al., 2003), however, the rate that slices diverged from whole liver was much lower in our experiments. High correlation (>0.8) to whole liver was maintained through day four in time course one and through day six in time courses two and three. Genes that are highly upregulated 24 hours after slicing were mostly enriched in signaling pathways (Fig. 2), likely related to repair and inflammatory response processes known to be triggered by physical liver damage that is unavoidable during the slicing process (Su et al., 2002). Since metabolic gene expression stabilizes after three days (Fig. 2, clusters 2 and 3), we used a three day recovery period for future metabolic studies so that changes in gene expression are more likely to be the result of the treatment rather than time. The gradual downward trend in co-expression correlation over time represents a slow drift in the global gene expression phenotype as opposed to a rapid gene expression change upon hepatocyte culturing. This is a known problem with hepatocyte cultures resulting from a combination of factors, especially the lack of circulating hormones produced elsewhere in the body causing time-dependent de-differentiation of hepatocytes (Elaut et al., 2006). Expression of liver marker genes was markedly higher in our liver slice culture than 2D hepatocyte culture (Fig. 5C) representing an improvement in long-term hepatocyte stability.

Exogenous ALA is taken up and triggers a liver-like response

ALA complexed with BCD was efficiently delivered to cells in a dose dependent manner. We observed a proportional increase in ALA and 20:3n-3 with increasing ALA concentration. While the ALA increase could be due to residual ALA sticking to the cells from the media, the proportional increase in 20:3n-3 with media ALA concentration supports active uptake and elongation of exogenous fatty acids (Fig. 4C). We did not observe any adverse effect of BCD on liver slices in any of our experiments, establishing the suitability of this delivery system for use in PCLS studies. There was no significant change in EPA or DHA after ALA supplementation. This does not mean that EPA and DHA are not being produced, but rather that the amount of ALA in the media is too low to cause a measurable increase in the already abundant pool of EPA and DHA in the cells. Indeed, both ALA and 20:3n-3 are low (0.88% and 0.35% respectively) in control slices, so a small increase in abundance could be detected. Future studies feeding radiolabeled ALA to liver slices are needed to confirm the production of DHA and EPA in PCLS.

ALA fed to slices has two fates within the PUFA biosynthesis pathway. The first and most common is the canonical pathway, where ALA is first desaturated by a Δ6 desaturase to 18:4n-3, then elongated and desaturated to EPA and DHA via Sprecher's shunt (Voss et al., 1991). The second occurs when ALA is first elongated to 20:3n-3, presumably by ELOVL5. In this case, a Δ8 desaturase is required to form 20:4n-3, which can then continue to EPA and DHA via the canonical pathway. This does however not happen efficiently in Atlantic salmon because of the low Δ8 desaturase activity of Δ6FADb (Monroig, Li & Tocher, 2011) in combination with low expression in liver (0.5-3.2 counts per million). Rather, 20:3n-3 accumulates in the cells or is catabolized for energy (Tocher, 2003), which is consistent with observations in feeding trials where fish fed vegetable oil based diets high in ALA contained higher tissue levels of 20:3n-3 (Tocher et al., 2001; Bell et al., 2010). This can explain why we measure increased levels of 20:3n-3, but not other PUFA intermediates.

We also observe that saturated fatty acids 16:0 and 18:0 increase between whole liver and liver slices. This agrees with the transcriptomic data where both fatty acid synthase genes, *fasa* and *fasb,* doubled (log2FC 1.08 and 1.02, respectively) in expression one day after slicing and the pathways "*fatty acid biosynthesis*" and "*glycerolipid metabolism*" were enriched in clusters that spike one day after slicing (clusters two and seven, Fig. 2C). Additionally, L15 is high in D+ galactose (5mM) and sodium pyruvate (5mM) providing an ample supply of acetate for *de novo* lipogenesis. Immediately after slice preparation, the tissue must recover by cellular repair and proliferation, which means there is a need for cell membranes that are composed of phospholipids rich in 16:0 and 18:0. These are synthesized *de novo* from fatty acid synthase and then incorporated into phospholipids through the glycerolipid and glycerophospholipid metabolism pathways (Vance & Vance, 2008). It is also possible that the 18:0 originates from FBS added to the media, however previous studies have found that FBS also contains high levels of 18:1n9 and we find that this decreases in liver slices (Stoll & Spector, 1984).

Overall, ALA concentration was positively correlated to lipid metabolism related gene expression, especially in PUFA biosynthesis with expression of all key pathway genes increasing with ALA. The same effect is known to occur in Atlantic salmon livers where fish fed vegetable oil-based diets high in ALA have higher PUFA biosynthesis gene expression relative to salmon fed fish oil-based diets low in ALA and high in EPA/DHA (Gillard et al., 2018). Additionally, this has been observed *in vitro* using Atlantic salmon primary hepatocytes (Kjær et al., 2016) and *in vivo* on rat liver (Tu et al., 2010). At very low concentration (20µM), expression of *Δ5fad*, *Δ6fada*, and *elovl5b* actually decreased relative to control slices with no ALA supplementation. In this experiment samples were taken two days after exposure to ALA, so it is possible that in 48 hours all of the ALA in the media was depleted, presumably taken up by the cells and anabolized to longer chain fatty acid products that have an inhibitory effect on expression. Additionally, the "*PPAR signaling pathway*", which includes PPARs and target genes, was significantly enriched in cluster three which increases with increasing ALA concentration (Fig. S1). PPARs are well known transcriptional factors that bind fatty acids and in turn activate genes involved in a wide range of cellular functions, most notably lipid metabolism (Poulsen, Siersbæk & Mandrup, 2012). Taken together our results demonstrate the ability of our PCLS model to accurately mimic expected shifts in lipid metabolism genes, highlighting its quality as an *in vitro* system.

Insulin triggers an anabolic response

Lipid metabolism, like other metabolic processes, is highly influenced by the feed status of the fish with insulin production triggered by feeding (Navarro et al., 2002). In order to ensure that the liver slices behaved similarly to liver in fed fish, we assessed the inclusion of insulin in the media. A main function of insulin is to shift the metabolic state from catabolic to anabolic, since it would be counterproductive for cells to actively produce energy by breaking down organic macromolecules while at the same time storing energy by building them up (Dimitriadis et al., 2011). In line with this we observe a binary response with several thousand genes either upregulated or downregulated in the presence of insulin, regardless of concentration (Fig. S2). Major anabolic pathways including "*biosynthesis of unsaturated fatty acids*" and "*fatty acid biosynthesis*" are upregulated in the presence of insulin in agreement with an anabolic response.

Physiological range for circulating insulin is 0.2-5nM (Caruso & Sheridan, 2011), so it is plausible that raising insulin concentrations to 100nM has little effect because all of the insulin receptors are likely bound at 10nM.

Insulin and ALA interact to regulate PUFA biosynthesis gene expression

Insulin and ALA displayed complex interaction effects on expression of genes related to PUFA biosynthesis in liver slices. Unaffected by ALA concentration, *elovl5a* and *elovl5b* were highly upregulated in the presence of insulin. On the other hand, genes that were upregulated in response to ALA tended to be upregulated in the presence of insulin alone, but then downregulated in the presence of insulin when combined with ALA (Fig. 4D). An important regulator of lipid metabolism in liver, sterol regulatory element binding protein 1 (*srebp-1*), is known to be upregulated by insulin through the PI3K/Akt/mTOR signaling pathway (Matsuzaka & Shimano, 2013), and indeed *srebp-1* is upregulated in response to insulin in our experiments. Both *elovl5a* and *elovl5b* contain sterol regulatory elements in their promoter regions (Carmona-Antoñanzas et al., 2013), and along with *Δ6fada* have been shown to increase in expression when co-transfected with *srebp-1* (Carmona-Antonanzas et al., 2014). On the other hand, activation of PPARα by ALA could work in opposition to insulin-mediated effects by stimulating beta-oxidation and ketogenesis. There is evidence in rats that Δ5 desaturase (D5D) and Δ6 desaturase (D6D) are under dual regulation by both SREBP-1 and PPARα (Matsuzaka et al., 2002), and given that regulation of lipid metabolism is highly conserved across species (Carmona-Antonanzas et al., 2014) it is likely a similar effect is present in salmon. The contrasting effect of insulin and ALA supplementation highlights the complex interplay between signaling networks balancing hormonal and nutritional input to optimize regulation of PUFA metabolism in Atlantic salmon.

Liver slices are more suitable for long-term culture than primary hepatocytes

We find that liver slices maintained liver-like gene expression patterns for longer than primary heptatocytes, which are generally known to undergo time-dependent de-differentiation (Elaut et al., 2006). We attribute this to the maintenance of the complex three-dimensional organization of whole liver with all interacting cell types. While hepatocytes are generally responsible for the metabolic activities associated with liver,

regulation of these functions is controlled in concert with nonparenchymal cells through complex endocrine and autocrine signaling networks (Kmiec, 2001). Eicosanoid signaling is a key component of these networks, which represents a layer of information that is completely lost in 2D hepatocyte cultures since eicosanoids are only produced in nonparenchymal cells (Johnston & Kroening, 1996). In mammals, glucose metabolism has been demonstrated to be influenced by nonparenchymal produced eicosanoids (Cherrington, 1999) and there is evidence that regulation of lipogenesis and PUFA metabolism is influenced by eicosanoid-mediated effects (Jump et al., 1999). In addition to eicosanoid production, interactions between hepatocytes and nonparenchymal cells are known to play a role in cell proliferation and differentiation (Kmiec, 2001) which could explain the higher liver slice culture expression of liver marker genes. This, along with many other factors likely contribute to the observed long-term differences between liver slice culture and 2D hepatocyte culture. Many of the metabolic processes in the liver are also regulated by circulating hormones produced in other parts of the body, so while liver slice culture is not identical to whole liver, we find that liver slice culture is better suited to long term metabolic studies than primary hepatocyte culture.

Conclusion

Taken together, our results demonstrate the utility and effectiveness of precision cut liver slices as a tool for studying lipid metabolism in Atlantic salmon. We found that when studying metabolism in liver slices, it is best to allow the slices to recover for three days before adding fatty acids, since gene expression in pathways relating to metabolism remains stable after three days in culture. Liver slices were highly responsive to both exogenous fatty acids and insulin in line with current understanding of lipid metabolism of Atlantic salmon. Supplementation with ALA induced expression of lipid metabolism genes and pathways while supplementation with insulin shifted gene expression to an anabolic state as expected. We also observed a different, sometimes opposing, regulatory effect of insulin and ALA on expression of genes involved in PUFA biosynthesis. Liver slices mimic the complex three dimensional structure of the liver and

453 produce results that are more relatable to liver *in vivo* than 2D hepatocyte culture. For this reason, liver
454 slices are an attractive alternative to 2D hepatocyte culture for interrogating metabolic pathways.
455

456 ## References

457 Anders S, Pyl PT, Huber W. 2015. HTSeq--a Python framework to work with high-throughput
458 sequencing data. *Bioinformatics* 31:166–169. DOI: 10.1093/bioinformatics/btu638.
459 Bell JG, Pratoomyot J, Strachan F, Henderson RJ, Fontanillas R, Hebard A, Guy DR, Hunter D, Tocher
460 DR. 2010. Growth, flesh adiposity and fatty acid composition of Atlantic salmon (Salmo salar)
461 families with contrasting flesh adiposity: Effects of replacement of dietary fish oil with vegetable
462 oils. *Aquaculture* 306:225–232. DOI: 10.1016/j.aquaculture.2010.05.021.
463 Bell JG, Tocher DR, Farndale BM, Cox DI, McKinney RW, Sargent JR. 1997. The effect of dietary lipid
464 on polyunsaturated fatty acid metabolism in Atlantic salmon (Salmo salar) undergoing parr-smolt
465 transformation. *Lipids* 32:515–525. DOI: 10.1007/s11745-997-0066-4.
466 Boess F, Kamber M, Romer S, Gasser R, Muller D, Albertini S, Suter L. 2003. Gene Expression in Two
467 Hepatic Cell Lines, Cultured Primary Hepatocytes, and Liver Slices Compared to the in Vivo Liver
468 Gene Expression in Rats: Possible Implications for Toxicogenomics Use of in Vitro Systems.
469 *Toxicological Sciences* 73:386–402. DOI: 10.1093/toxsci/kfg064.
470 Brunaldi K, Huang N, Hamilton JA. 2010. Fatty acids are rapidly delivered to and extracted from
471 membranes by methyl-beta-cyclodextrin. *Journal of lipid research* 51:120–31. DOI:
472 10.1194/M900200-JLR200.
473 Carmona-Antonanzas G, Tocher DR, Martinez-Rubio L, Leaver MJ. 2014. Conservation of lipid
474 metabolic gene transcriptional regulatory networks in fish and mammals. *Gene* 534:1–9. DOI:
475 10.1016/j.gene.2013.10.040.
476 Carmona-Antoñanzas G, Tocher DR, Taggart JB, Leaver MJ. 2013. An evolutionary perspective on
477 Elovl5 fatty acid elongase: comparison of Northern pike and duplicated paralogs from Atlantic
478 salmon. *BMC Evolutionary Biology* 13:85. DOI: 10.1186/1471-2148-13-85.

479 Caruso MA, Sheridan MA. 2011. New insights into the signaling system and function of insulin in fish.
480 *General and Comparative Endocrinology* 173:227–247. DOI: 10.1016/j.ygcen.2011.06.014.
481 Cherrington AD. 1999. Control of glucose uptake and release by the liver in vivo. *Diabetes* 48:1198–214.
482 DOI: 10.2337/DIABETES.48.5.1198.
483 Dimitriadis G, Mitrou P, Lambadiari V, Maratou E, Raptis SA. 2011. Insulin effects in muscle and
484 adipose tissue. *Diabetes Research and Clinical Practice* 93:S52–S59. DOI: 10.1016/S0168-
485 8227(11)70014-6.
486 Dobin A, Davis CA, Schlesinger F, Drenkow J, Zaleski C, Jha S, Batut P, Chaisson M, Gingeras TR.
487 2013. STAR: Ultrafast universal RNA-seq aligner. *Bioinformatics* 29:15–21. DOI:
488 10.1093/bioinformatics/bts635.
489 Eide M, Karlsen OA, Kryvi H, Olsvik PA, Goksøyr A. 2014. Precision-cut liver slices of Atlantic cod
490 (Gadus morhua): An in vitro system for studying the effects of environmental contaminants. *Aquatic*
491 *Toxicology* 153:110–115. DOI: 10.1016/j.aquatox.2013.10.027.
492 Ekins S. 1996. Past, Present, and Future Applications of Precision-Cut Liver Slices for in Vitro
493 Xenobiotic Metabolism. *Drug Metabolism Reviews* 28:591–623. DOI:
494 10.3109/03602539608994019.
495 Elaut G, Henkens T, Papeleu P, Snykers S, Vinken M, Vanhaecke T, Rogiers V. 2006. Molecular
496 Mechanisms Underlying the Dedifferentiation Process of Isolated Hepatocytes and Their Cultures.
497 *Current Drug Metabolism* 7:629–660. DOI: 10.2174/138920006778017759.
498 Fortin É, Blouin R, Lapointe J, Petit H V., Palin M-F. 2017. Linoleic acid, α-linolenic acid and
499 enterolactone affect lipid oxidation and expression of lipid metabolism and antioxidant-related genes
500 in hepatic tissue of dairy cows. *British Journal of Nutrition* 117:1199–1211. DOI:
501 10.1017/S0007114517000976.
502 Gillard G, Harvey TN, Gjuvsland A, Jin Y, Thomassen M, Lien S, Leaver M, Torgersen JS, Hvidsten TR,
503 Vik JO, Sandve SR. 2018. Life-stage-associated remodelling of lipid metabolism regulation in
504 Atlantic salmon. *Molecular Ecology* 27:1200–1213. DOI: 10.1111/mec.14533.

505 Janssen AWF, Betzel B, Stoopen G, Berends FJ, Janssen IM, Peijnenburg AA, Kersten S. 2015. The
506 impact of PPARα activation on whole genome gene expression in human precision cut liver slices.
507 *BMC Genomics* 16:760. DOI: 10.1186/s12864-015-1969-3.
508 Johnston DE, Kroening C. 1996. Stimulation of prostaglandin synthesis in cultured liver cells by CCl4.
509 *Hepatology* 24:677–684. DOI: 10.1002/hep.510240334.
510 Jump D., Thelen A, Ren B, Mater M. 1999. Multiple mechanisms for polyunsaturated fatty acid
511 regulation of hepatic gene transcription. *Prostaglandins, Leukotrienes and Essential Fatty Acids*
512 60:345–349. DOI: 10.1016/S0952-3278(99)80010-6.
513 Kjær MA, Ruyter B, Berge GM, Sun Y, Østbye T-KK. 2016. Regulation of the Omega-3 Fatty Acid
514 Biosynthetic Pathway in Atlantic Salmon Hepatocytes. *PloS one* 11:e0168230. DOI:
515 10.1371/journal.pone.0168230.
516 Kmiec Z. 2001. Cooperation of Liver Cells in Health and Disease. DOI: 10.1007/978-3-642-56553-3_7.
517 Krumdieck CL, Dos Santos JE, Ho K-J. 1980. A new instrument for the rapid preparation of tissue slices.
518 *Analytical Biochemistry* 104:118–123. DOI: 10.1016/0003-2697(80)90284-5.
519 Leaver MJ, Bautista JM, Björnsson BT, Jönsson E, Krey G, Tocher DR, Torstensen BE. 2008. Towards
520 Fish Lipid Nutrigenomics : Current State and Prospects for Fin-Fish Aquaculture. *Reviews in*
521 *Fisheries Science* 16:73–94. DOI: 10.1080/10641260802325278.
522 Matsuzaka T, Shimano H. 2013. Insulin-dependent and -independent regulation of sterol regulatory
523 element-binding protein-1c. *Journal of diabetes investigation* 4:411–2. DOI: 10.1111/jdi.12098.
524 Matsuzaka T, Shimano H, Yahagi N, Amemiya-Kudo M, Yoshikawa T, Hasty AH, Tamura Y, Osuga J,
525 Okazaki H, Iizuka Y, Takahashi A, Sone H, Gotoda T, Ishibashi S, Yamada N. 2002. Dual
526 regulation of mouse Delta(5)- and Delta(6)-desaturase gene expression by SREBP-1 and
527 PPARalpha. *Journal of lipid research* 43:107–14.
528 Monroig Ó, Li Y, Tocher DR. 2011. Delta-8 desaturation activity varies among fatty acyl desaturases of
529 teleost fish: High activity in delta-6 desaturases of marine species. *Comparative Biochemistry and*
530 *Physiology Part B: Biochemistry and Molecular Biology* 159:206–213. DOI:

10.1016/J.CBPB.2011.04.007.

Navarro I, Rojas P, Capilla E, Albalat A, Castillo J, Montserrat N, Codina M, Gutiérrez J. 2002. Insights into Insulin and Glucagon Responses in Fish. *Fish Physiology and Biochemistry* 27:205–216. DOI: 10.1023/B:FISH.0000032726.78074.04.

Neyrinck AM, Gomez C, Delzenne NM. 2004. Precision-cut liver slices in culture as a tool to assess the physiological involvement of Kupffer cells in hepatic metabolism. *Comparative hepatology* 3 Suppl 1:S45. DOI: 10.1186/1476-5926-2-S1-S45.

O'Fallon J V., Busboom JR, Nelson ML, Gaskins CT. 2007. A direct method for fatty acid methyl ester synthesis: Application to wet meat tissues, oils, and feedstuffs. *Journal of Animal Science* 85:1511–1521. DOI: 10.2527/jas.2006-491.

Poulsen L la C, Siersbæk M, Mandrup S. 2012. PPARs: Fatty acid sensors controlling metabolism. *Seminars in Cell & Developmental Biology* 23:631–639. DOI: 10.1016/J.SEMCDB.2012.01.003.

Robinson MD, McCarthy DJ, Smyth GK. 2010. edgeR: a Bioconductor package for differential expression analysis of digital gene expression data. *Bioinformatics (Oxford, England)* 26:139–40. DOI: 10.1093/bioinformatics/btp616.

Starokozhko V, Abza GB, Maessen HC, Merema MT, Kuper F, Groothuis GMM. 2015. Viability, function and morphological integrity of precision-cut liver slices during prolonged incubation: Effects of culture medium. *Toxicology in Vitro* 30:288–299. DOI: 10.1016/j.tiv.2015.10.008.

Stoll LL, Spector AA. 1984. Changes in serum influence the fatty acid composition of established cell lines. *In Vitro* 20.

Su AI, Guidotti LG, Pezacki JP, Chisari F V, Schultz PG. 2002. Gene expression during the priming phase of liver regeneration after partial hepatectomy in mice. *Proceedings of the National Academy of Sciences of the United States of America* 99:11181–6. DOI: 10.1073/pnas.122359899.

Szalowska E, van der Burg B, Man H-Y, Hendriksen PJM, Peijnenburg AACM. 2014. Model Steatogenic Compounds (Amiodarone, Valproic Acid, and Tetracycline) Alter Lipid Metabolism by Different Mechanisms in Mouse Liver Slices. *PLoS ONE* 9:e86795. DOI: 10.1371/journal.pone.0086795.

557 Tocher DR. 2003. Metabolism and Functions of Lipids and Fatty Acids in Teleost Fish. *Reviews in*
558 *Fisheries Science* 11:107–184. DOI: 10.1080/713610925.
559 Tocher DR, Bell JG, MacGlaughlin P, McGhee F, Dick JR. 2001. Hepatocyte fatty acid desaturation and
560 polyunsaturated fatty acid composition of liver in salmonids: effects of dietary vegetable oil.
561 *Comparative Biochemistry and Physiology Part B: Biochemistry and Molecular Biology* 130:257–
562 270. DOI: 10.1016/S1096-4959(01)00429-8.
563 Tu WC, Cook-Johnson RJ, James MJ, Mühlhäusler BS, Gibson RA. 2010. Omega-3 long chain fatty acid
564 synthesis is regulated more by substrate levels than gene expression. *Prostaglandins, Leukotrienes*
565 *and Essential Fatty Acids* 83:61–68. DOI: 10.1016/J.PLEFA.2010.04.001.
566 Vance DE, Vance JE. 2008. Phospholipid biosynthesis in eukaryotes. *Biochemistry of Lipids,*
567 *Lipoproteins and Membranes*:213–244. DOI: 10.1016/B978-044453219-0.50010-6.
568 Vancha AR, Govindaraju S, Parsa KV, Jasti M, González-García M, Ballestero RP. 2004. Use of
569 polyethyleneimine polymer in cell culture as attachment factor and lipofection enhancer. *BMC*
570 *Biotechnology* 4:23. DOI: 10.1186/1472-6750-4-23.
571 Voss A, Reinhart M, Sankarappa S, Sprecher H. 1991. The metabolism of 7,10,13,16,19-
572 docosapentaenoic acid to 4,7,10,13,16,19-docosahexaenoic acid in rat liver is independent of a 4-
573 desaturase. *Journal of Biological Chemistry* 266:19995–20000.
574 Wake K, Sato T. 2015. “The Sinusoid” in the Liver: Lessons Learned from the Original Definition by
575 Charles Sedgwick Minot (1900). *The Anatomical Record* 298:2071–2080. DOI: 10.1002/ar.23263.
576 Warburg O. 1923. Versuche an überlebendem Karzinomgewebe. *Bioche- mische Zeitschrift* 142:317–333.
577 Wu X, Roberto JB, Knupp A, Kenerson HL, Truong CD, Yuen SY, Brempelis KJ, Tuefferd M, Chen A,
578 Horton H, Yeung RS, Crispe IN. 2018. Precision-cut human liver slice cultures as an immunological
579 platform. *Journal of Immunological Methods* 455:71–79. DOI: 10.1016/J.JIM.2018.01.012.
580

Figure 1

Viability and morphology of liver slices.

(A) Confocal scanning laser microscope (CLSM) image of a liver slice. Cells are stained with Hoechst (blue) and dead cells with propidium iodide (red). (B) Cell viability when incubated in media (none) and media supplemented with alpha-linolenic acid (ALA), insulin (INS), empty methyl-β-cyclodextrin (BCD), or a combination as measured by CLSM live/dead counts. Points represent viability measurements from a single liver slice. (C) Cross sections of paraffin embedded liver slice sampled at day zero (immediately after slicing), day three, and day five. The sections were stained with hematoxylin and eosin and photographed using light microscopy at 20x magnification. Scale bars are 100μM in length.

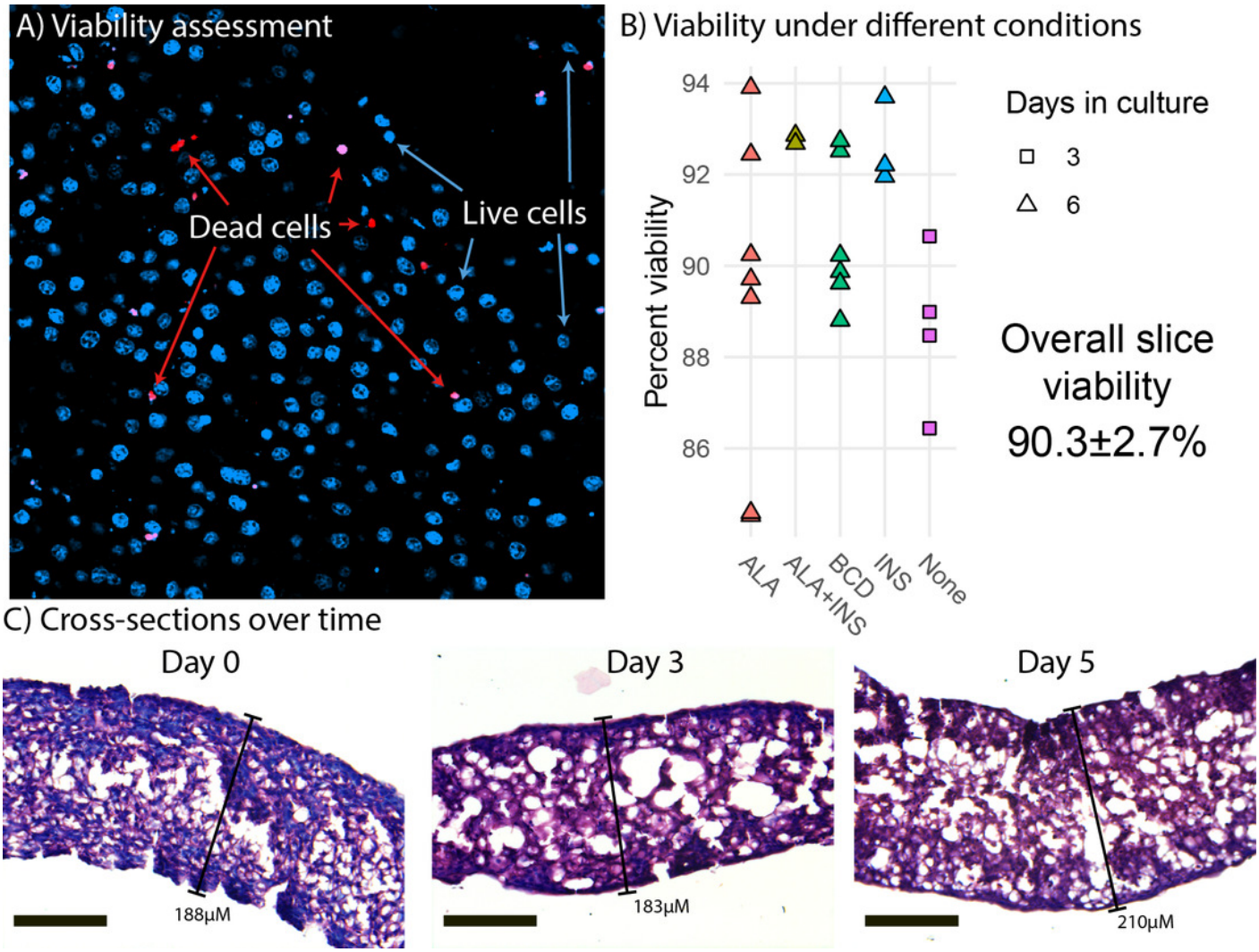
A) Viability assessment
Dead cells
Live cells
B) Viability under different conditions
Percent viability
94
92
90
88
86
ALA
ALA+INS
BCD
INS
None
Days in culture
3
6
Overall slice viability
90.3±2.7%
C) Cross-sections over time
Day 0
188µM
Day 3
183µM
Day 5
210µM

Figure 2

Global gene expression patterns over time.

A) Heatmap showing changes in the liver slice transcriptome over time. Heatmap includes 16,267 genes significantly differentially expressed (FDR <0.01, log2FC >1) over the course of 9 days. Each time point was measured in triplicate. Transcript abundance is expressed in counts per million and were individually scaled across days to highlight changes in gene expression. B) Genes behaving similarly over time were clustered using Ward's method and broken into eight groups. Trend lines are based on mean scaled values in each cluster. C) KEGG pathway enrichment analysis was run on each cluster to determine how the liver slices are changing over time. Each point represents a significantly enriched pathway (p <0.001).

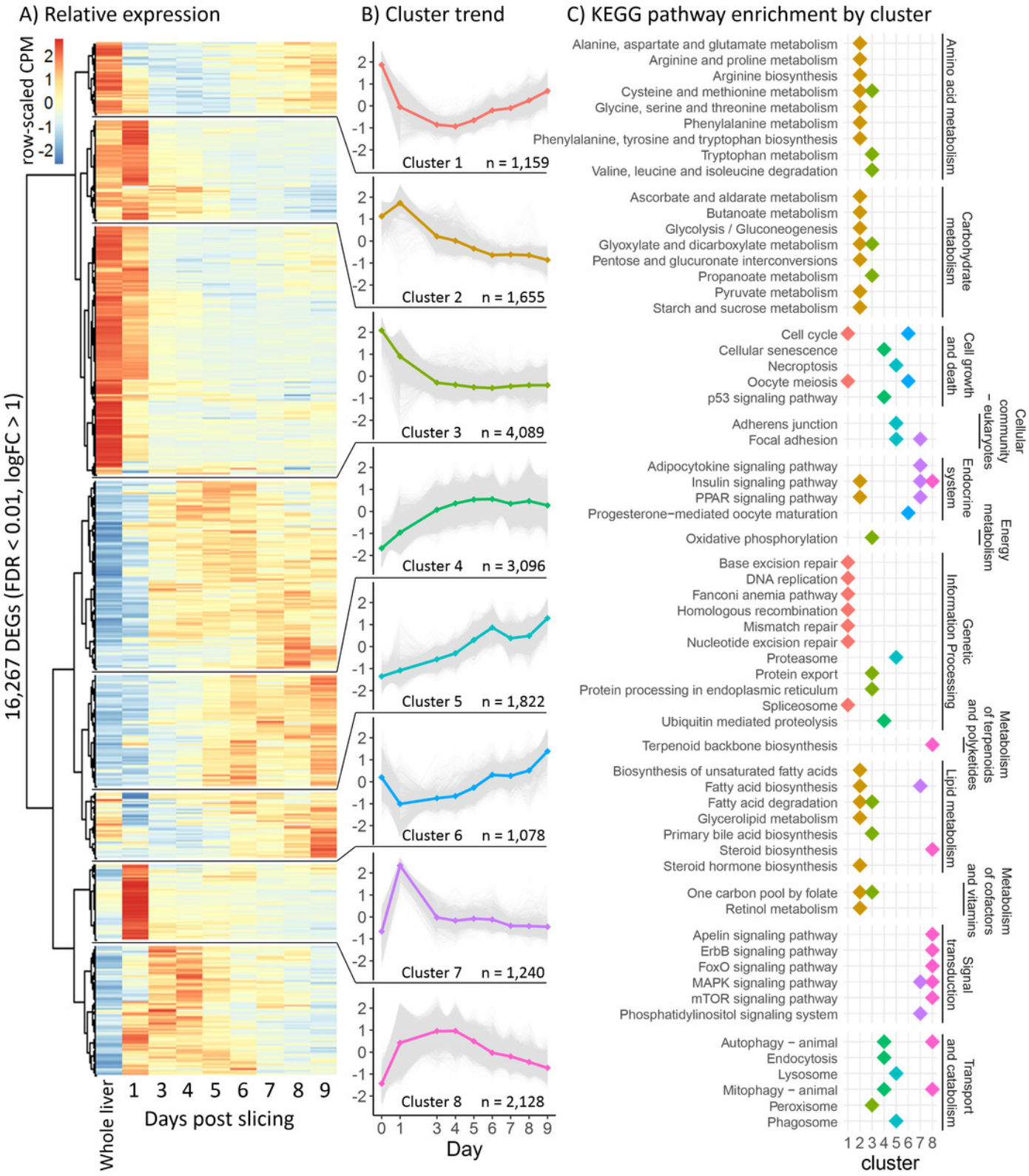
A) Relative expression
B) Cluster trend
C) KEGG pathway enrichment by cluster
row-scaled CPM
16,267 DEGs (FDR < 0.01, logFC > 1)
Whole liver
Days post slicing
Cluster 1 n = 1,159
Cluster 2 n = 1,655
Cluster 3 n = 4,089
Cluster 4 n = 3,096
Cluster 5 n = 1,822
Cluster 6 n = 1,078
Cluster 7 n = 1,240
Cluster 8 n = 2,128
Day
Alanine, aspartate and glutamate metabolism
Arginine and proline metabolism
Arginine biosynthesis
Cysteine and methionine metabolism
Glycine, serine and threonine metabolism
Phenylalanine metabolism
Phenylalanine, tyrosine and tryptophan biosynthesis
Tryptophan metabolism
Valine, leucine and isoleucine degradation
Amino acid metabolism
Ascorbate and aldarate metabolism
Butanoate metabolism
Glycolysis / Gluconeogenesis
Glyoxylate and dicarboxylate metabolism
Pentose and glucuronate interconversions
Propanoate metabolism
Pyruvate metabolism
Starch and sucrose metabolism
Carbohydrate metabolism
Cell cycle
Cellular senescence
Necroptosis
Oocyte meiosis
p53 signaling pathway
Cell growth and death
Adherens junction
Focal adhesion
Cellular community – eukaryotes
Adipocytokine signaling pathway
Insulin signaling pathway
PPAR signaling pathway
Progesterone−mediated oocyte maturation
Endocrine system
Oxidative phosphorylation
Energy metabolism
Base excision repair
DNA replication
Fanconi anemia pathway
Homologous recombination
Mismatch repair
Nucleotide excision repair
Proteasome
Protein export
Protein processing in endoplasmic reticulum
Spliceosome
Ubiquitin mediated proteolysis
Genetic Information Processing
Terpenoid backbone biosynthesis
Metabolism of terpenoids and polyketides
Biosynthesis of unsaturated fatty acids
Fatty acid biosynthesis
Fatty acid degradation
Glycerolipid metabolism
Primary bile acid biosynthesis
Steroid biosynthesis
Steroid hormone biosynthesis
Lipid metabolism
One carbon pool by folate
Retinol metabolism
Metabolism of cofactors and vitamins
Apelin signaling pathway
ErbB signaling pathway
FoxO signaling pathway
MAPK signaling pathway
mTOR signaling pathway
Phosphatidylinositol signaling system
Signal transduction
Autophagy − animal
Endocytosis
Lysosome
Mitophagy − animal
Peroxisome
Phagosome
Transport and catabolism
cluster

Figure 3(on next page)

Co-expression correlation of liver slices over time for select lipid metabolism pathways.

Co-expression correlations (Spearman) between mean whole liver expression and gene expression from different days in time course one (red), time course two (green), and time course three (blue). Experiments use data from liver slices in triplicate each day. Experiments were divided by insulin and media change regime. Time course two and three contained insulin, time course one and three had media changed every three days, and time course two had media changed daily. Correlations were calculated for all expressed genes (top left) and genes from seven lipid metabolism pathways.

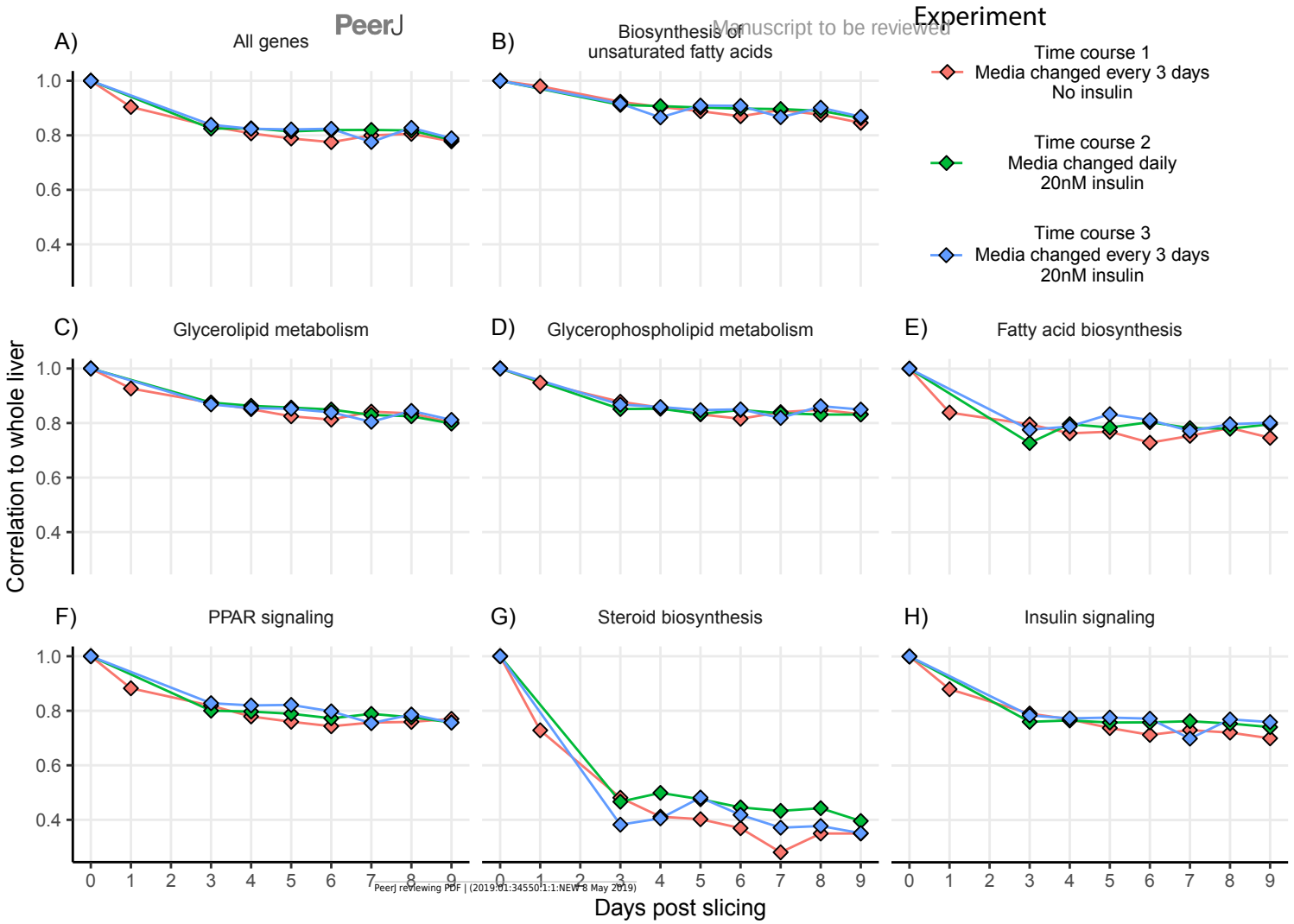

Figure 4(on next page)

Effect of ALA and insulin on PUFA biosynthesis in liver slices.

A) Schematic diagram of the polyunsaturated fatty acid biosynthesis (PUFA) biosynthesis pathway. B) Gene-scaled log counts per million (CPM) of PUFA biosynthesis genes with increasing alpha-linolenic acid (ALA) concentration. C) Gene-scaled logCPM of PUFA biosynthesis genes with increasing insulin concentration with and without ALA supplementation. D) Relative abundance of ALA, 20:3n3, eicosapentaenoic acid, and docosahexaenoic acid with increasing ALA concentration. For all plots, large square, diamond, or circle points show mean scaled values of triplicate slices (logCPM or percent fatty acid) while small points show scaled values of individual replicates. Point size corresponds to unscaled values (logCPM or percent fatty acid) of the mean. Letters indicate significant ($q<0.05$) differences between groups (ALA or insulin concentration) for corresponding genes or fatty acids.

A) PUFA biosynthesis pathway

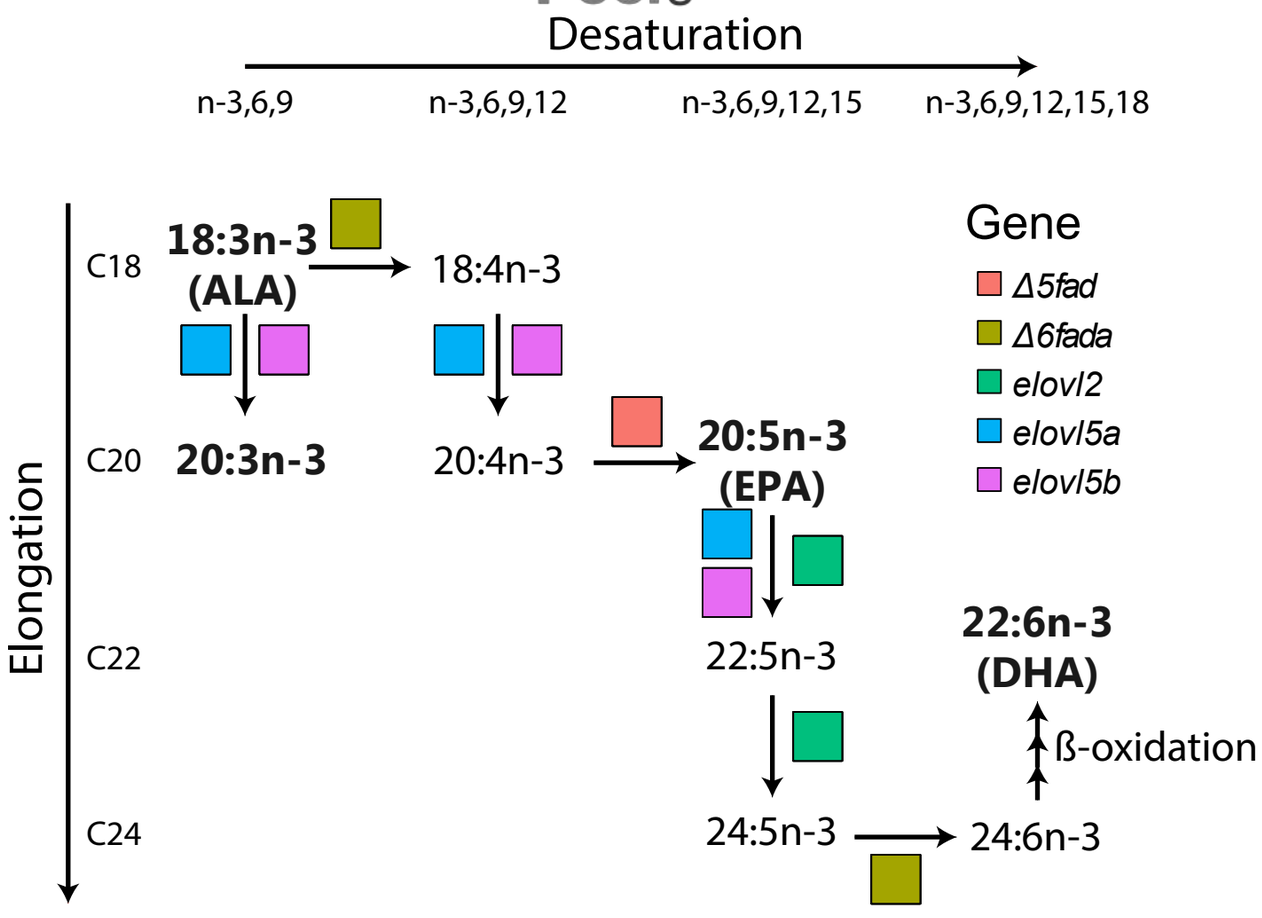

B) Expression response to ALA supplementation

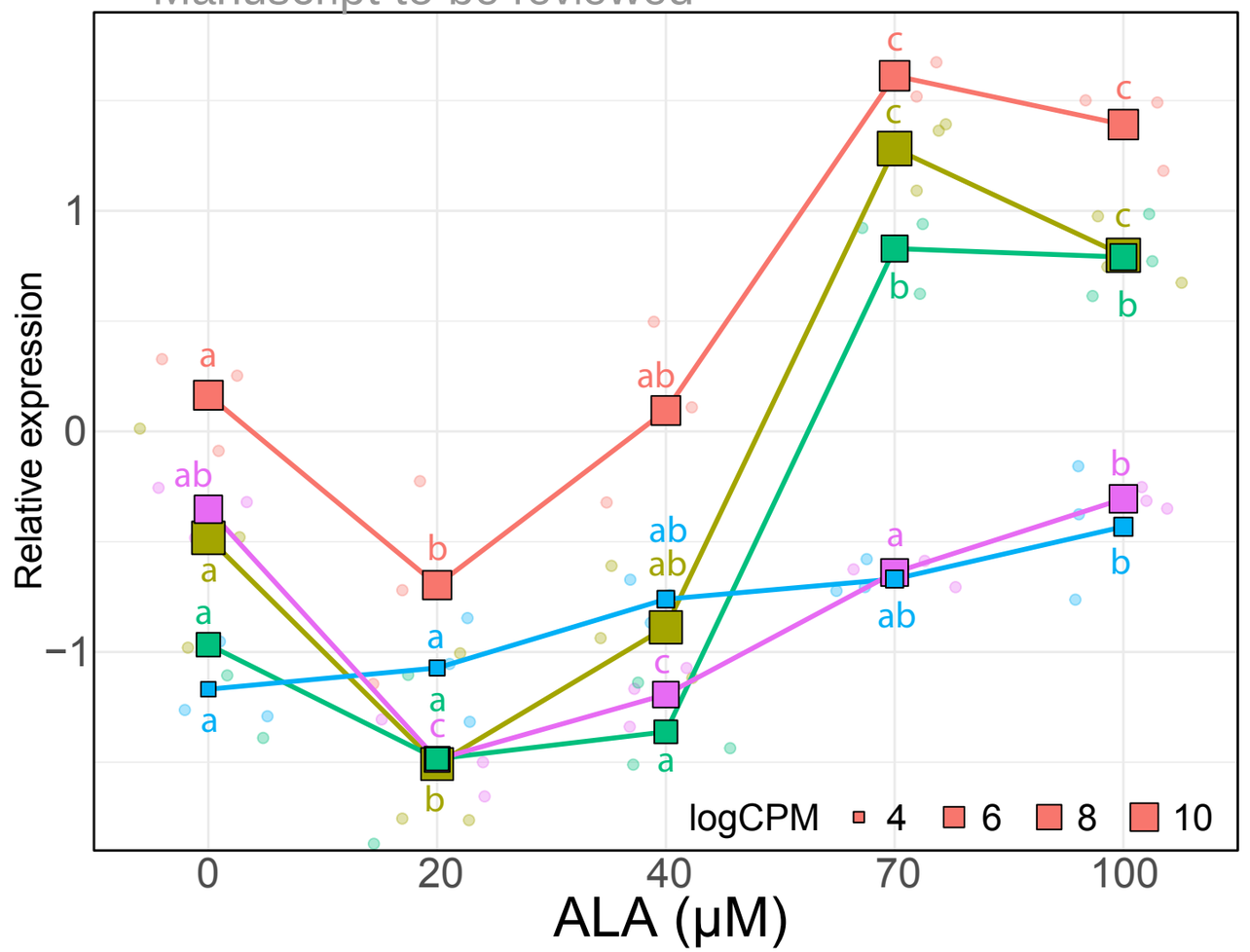

C) Fatty acid shifts from ALA supplementation

D) Expression interaction between ALA and insulin

Figure 5(on next page)

Expression of select pathways and genes in hepatocyte culture, liver slice culture, and whole liver.

Transcriptomic data from each source was pooled to give a range of possible gene expression levels (hepatocyte culture n = 16, liver slice culture n = 89, whole liver n = 210) A) Relative expression profiles for five selected lipid metabolism pathways. Values are expressed mean scaled log2 CPM of all genes within a pathway for each sample with a minimum CPM of 1. B) Relative expression of key genes in the PUFA biosynthesis pathway with a minimum CPM of 10. Abbreviations:*Δ6fad*= delta-6 fatty acid desaturase,*elovl5*= fatty acid elongase 5,*Δ5fad*= delta-5 fatty acid desaturase,*elovl2*= fatty acid elongase 2. C) Relative expression of select liver marker genes with a minimum CPM of 10. Abbreviations:*alb*= albumin,*g6pcl*= glucose-6-phosphatase-like,*tatl*= tyrosine aminotransferase-like,*cyp3al*= cytochrome P450 3A27-like,*pck1*= phosphoenolpyruvate carboxykinase 1,*tdo2*= tryptophan 2,3-dioxygenase,*tod2l*= tryptophan 2,3-dioxygenase-like.